

Guanosine oxidation explored by pulse radiolysis coupled with transient electrochemistry.

A. Latus,^{a,b} M. S. Alam,^{a,b} M. Mostafavi,^c J-L. Marignier*^c and E. Maisonhaute*^{a,b}

^a Sorbonne Universités, UPMC Univ Paris 06, UMR 8235, Laboratoire Interfaces et Systèmes Electrochimiques, F-75005 Paris, France. e-mail: emmanuel.maisonhaute@upmc.fr

^b Sorbonne Universités, CNRS, UMR 8235, Laboratoire Interfaces et Systèmes Electrochimiques, F-75005 Paris, France.

^c Laboratoire de Chimie Physique, CNRS UMR 8000, Université Paris-Sud, Bat 350, 91405 Orsay Cedex, France. e-mail: jean-louis.marignier@u-psud.fr.

Electronic Supplementary Information

Experimental Section

Guanosine, guanosinemonophosphate, KBr (Aldrich) and N₂O gas were used without further purification.

The electrochemical set-up was identical compared to our previous paper,¹ excepted that we placed the reference electrode (AgCl/Ag, saturated KCl, Orignalys) in a separate compartment. Both compartments were connected with a salt bridge containing 2M KCl in agar-agar. The working electrode was a melted gold ball cleaned by passing it in a butane flame prior the experiment. Its area was evaluated to $6.6 \times 10^{-3} \text{ cm}^2$ by calibration in an aqueous 1 mM ferrocenemethanol (Aldrich) solution. The counter electrode was a Pt wire.

Experiments were run at ELYSE electron accelerator at 22 °C. Transient spectra were recorded with a Hamamatsu C7700 streak camera that allows one to record simultaneously the transient absorption spectra from 250 to 850 nm and its time evolution in temporal windows from 500 ps to 1 ms with a time resolution of 4 ps. Initial concentration of radicals produced by the radiolytic pulse was calculated before each experiment by measuring the absorbance of hydrated electrons at 660 nm and 3 ns after the pulse in a water reference cell with a value of the extinction coefficient $\epsilon_{660\text{nm}} \approx 18,000 \text{ M}^{-1} \text{ cm}^{-1}$. We considered that all reducing species (e^-_{aq} and H^\bullet) were all quenched by N₂O and converted to OH^\bullet thus doubling the initial concentration of OH^\bullet . They were then quantitatively converted to $\text{Br}_2^{\bullet-}$ and finally to $\mathbf{G(-H)}^\bullet$, allowing the initial starting concentration of $\mathbf{G(-H)}^\bullet$ to be known.

In the electrochemical experiment, an intense parasitic spike is observed initially when the electron pulse exits the accelerator. This spike is observed also if the electrochemical cell is placed outside the electron beam. We believe that it is due to a transient destabilization of the potentiostat loop. This spike obtained outside the cell can be subtracted from the signal obtained when the electron beam is directed onto the electrode to obtain the faradaic signal only. At each potential and for each position of the electrode (outside or inside the electron beam), about 10 transients were acquired and then averaged for both signals in order to obtain the transients presented in figure 2 of the main text. Figure S1 presents an example of both signals at 501 mV vs AgCl/Ag.

Simulations of the reconstructed polarograms were implemented with Matlab®. The simulations of the transients were performed with Digielch® using the chronoamperometry method but deactivating the pre-equilibrium possibility.

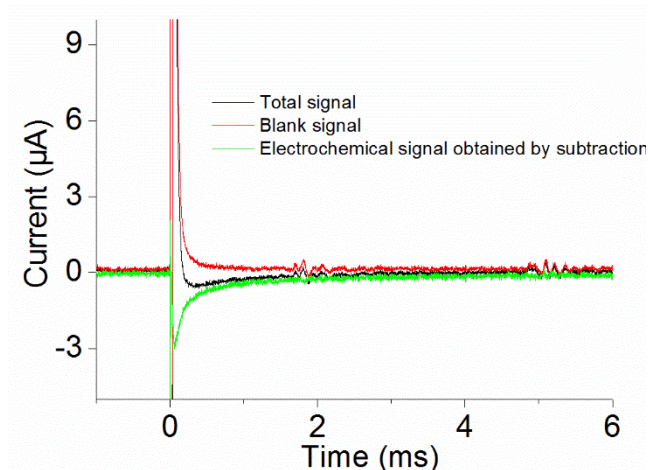


Figure S1. Transients observed when the electrochemical cell was placed outside the electron beam (red) or when the electrode was placed on the beam trajectory (black). Faradaic signal obtained by subtraction (green). Potential 501 mV vs. AgCl/Ag. Solution composition: 1 mM guanosine, 0.1 M KBr, 0.1 M phosphate buffer under N₂O saturation. Dose: 38 Gy/pulse (28 µM initial concentration in **G(-H)•**). pH = 7.1.

Simulation of experimental transients

1. Diffusion limited current I_{lim}

In a first stage, for potentials more negative than 400 mV vs AgCl/Ag, only reduction of the radical **G(-H)•** can be considered since the reduction rate is much faster than the oxidation one. Without any chemical reaction, the current would then follow the Cottrell equation.¹⁻³ However, since a bimolecular reaction decay occurs in solution in the case of guanosine, this is not any more the case here. The limiting current I_{lim} corresponds to the flux towards the electrode according to:

$$\frac{I_{lim}(t)}{FA} = -D \frac{\partial[G(-H)•]_{x=0}}{\partial x} \quad (S1)$$

with $[G(-H)•]_{x=0} = 0$. However, additionally disappearance of **G(-H)•** in solution should be taken into account by:

$$\frac{\partial[G(-H)•]}{\partial t} = -k_{SO}[G(-H)•]^2 \quad (S2)$$

There is to the best of our knowledge no analytical solution for this situation but knowing the initial concentration of **G(-H)•**, the diffusion coefficient^{4, 5} of guanosine ($D = 7 \times 10^{-10} \text{ m}^2\text{s}^{-1}$) and the electrode area, we could rely on digital simulations to solve equations (S1) and (S2). Here, the only adjustable parameter was the kinetic rate constant k_{SO} . Figure S2 presents the fits obtained with $k_{SO} = 0 ; 2 \times 10^7 ; 3 \times 10^7 ; 4 \times 10^7$ and $10^9 \text{ M}^{-1}\text{s}^{-1}$.

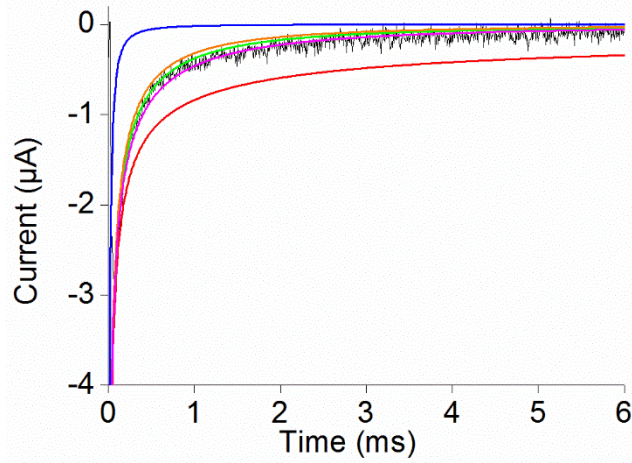


Figure S2. Experimental reduction current obtained at 401 mV vs AgCl/Ag (black) and corresponding simulations for $k_{SO} = 0$ (red); 2×10^7 (pink); 3×10^7 (green); 4×10^7 (orange) and 10^9 (blue) $M^{-1}s^{-1}$. Solution composition: 1 mM guanosine, 0.1 M KBr, 0.1 M phosphate buffer under N_2O saturation. Dose: 38 Gy/pulse (28 μM initial concentration in $G(-H)^\bullet$). pH = 7.1.

The best agreement between theory and experiment was found for $k_{SO} = 3 \times 10^7 M^{-1}s^{-1}$ and this value was then taken as input for the following experimental fits at intermediate potentials.

2. Simulation at intermediate potentials

In the general case, the competition between oxidation and reduction at the electrode surface needs to be taken into account according to equation (1) of the main text. In the present study, the potentials explored are sufficiently far from the standard potentials so that even with rate constants near $1 \text{ cm}^2\text{s}^{-1}$, irreversible and not Nernstian electron transfer need to be considered. But apart from usual electrochemical systems, since electron transfers occur far from the apparent standard potentials, the electron transfer rates for either oxidation or reduction are very fast. Therefore, for any potential, the concentration of $G(-H)^\bullet$ at the electrode surface is 0 and the flux of $G(-H)^\bullet$ towards the electrode remains unchanged and identical to the one on the limiting plateau. We then expect the concentration dependence of $G(-H)^\bullet$ to the electrode distance to be identical at all potentials. This justifies that the procedure described in ref 25 of the main text elaborated for systems where no reaction occurred in solution can be adapted to our study.

The oxidative contribution of the current I_{ox} is then given by:

$$\frac{I_{ox}}{FA} = \frac{-k_{ox}}{k_{ox} + k_{red}} \times \frac{I_{lim}}{FA} \quad (S3)$$

$$\text{and } \frac{I_{red}}{FA} = \frac{k_{red}}{k_{ox} + k_{red}} \times \frac{I_{lim}}{FA} \quad (S4)$$

is obtained for the reductive contribution.

Finally, the current $I = I_{ox} + I_{red}$ can then be expressed as:

$$I = I_{lim} \times \frac{k_{ox} - k_{red}}{k_{ox} + k_{red}} \quad (S5)$$

where k_{ox} and k_{red} can be expressed by equations (2-5) of the main text. Since the ratio of the rate constant appears in equation S5, the precise values of k_{ox}^0 and k_{red}^0 are not influencing I as long as they are large enough to allow efficient electron transfers. For example, at 621 mV vs AgCl/Ag we observed absolutely no changes in the simulated decay as long as k_{ox}^0 and k_{red}^0

were equal and larger than 10^{-3} cm^{-1} (keeping $\lambda_{\text{ox}} = \lambda_{\text{red}} = 0.9 \text{ eV}$). However, the value $k_{\text{ox}}^0/k_{\text{red}}^0$ plays a major role in the switch between positive and negative current, as well as the value of $\lambda_{\text{ox}}/\lambda_{\text{red}}$.

Complementary spectroscopic and electrochemical data

The noise in the data acquired for guanosine was more important both for spectroscopic and electrochemistry experiments. In fact experiments for guanosine monophosphate were performed after those for guanosine, which allowed an optimization of the settings of the electron accelerator and position of the current sensor of the potentiostat.

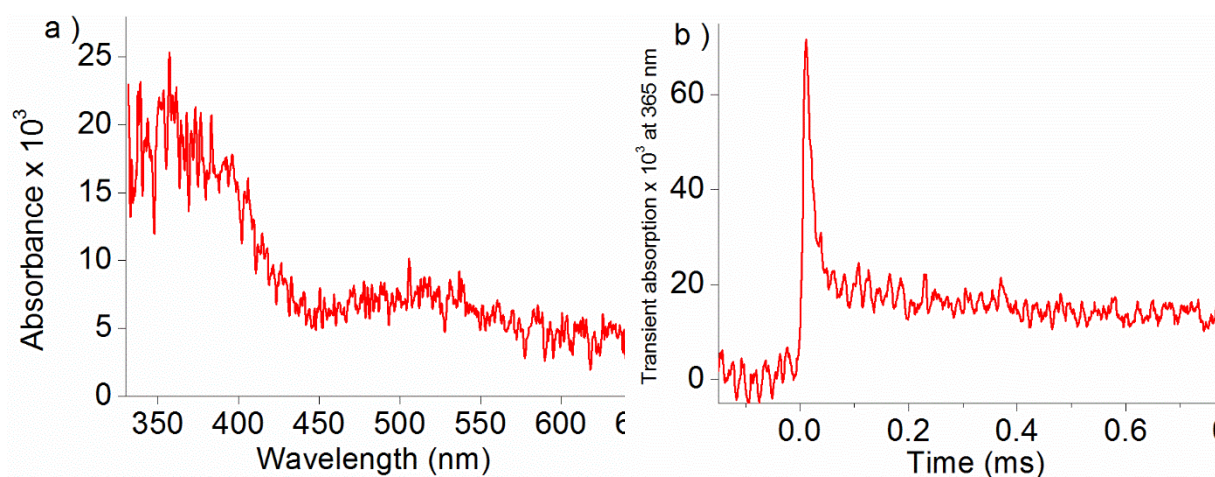


Figure S3. Transient spectroscopy of a 1 mM guanosine solution upon oxidation by $\text{Br}_2^{\bullet-}$. a) Transient spectrum observed 80 μs after the pulse. b) Transient absorption at 365 nm.

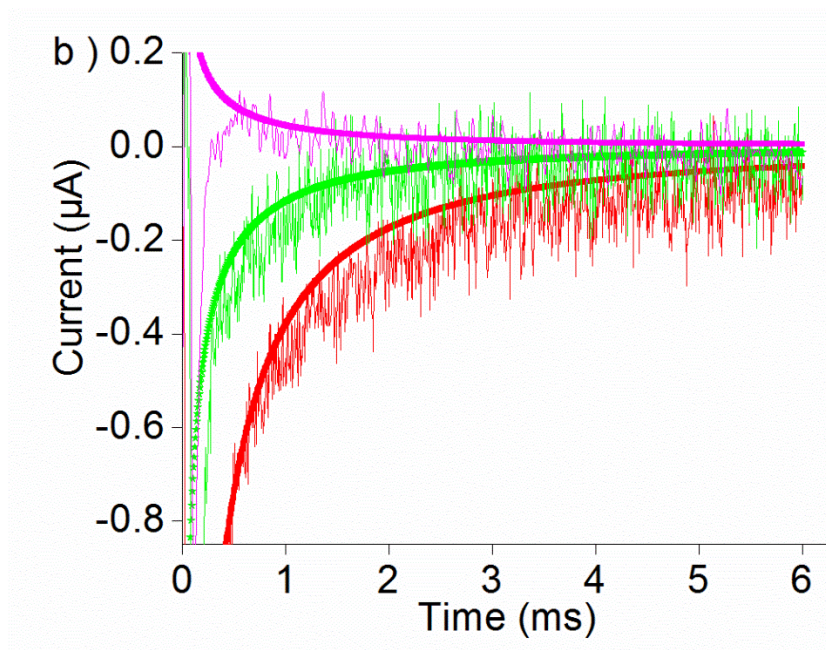


Figure S4. Oxidation of guanosine by $\text{Br}_2^{\bullet-}$. Transient experimental and simulated electrochemical currents recorded at different potentials vs AgCl/Ag : 401 mV (red), 582 mV (blue), 621 mV (green) and 641 mV (magenta). Solution composition: 1 mM guanosine, 0.1 M KBr, 0.1 M phosphate buffer under N_2O saturation. Dose: 38 Gy/pulse. Here the raw data were not filtered.

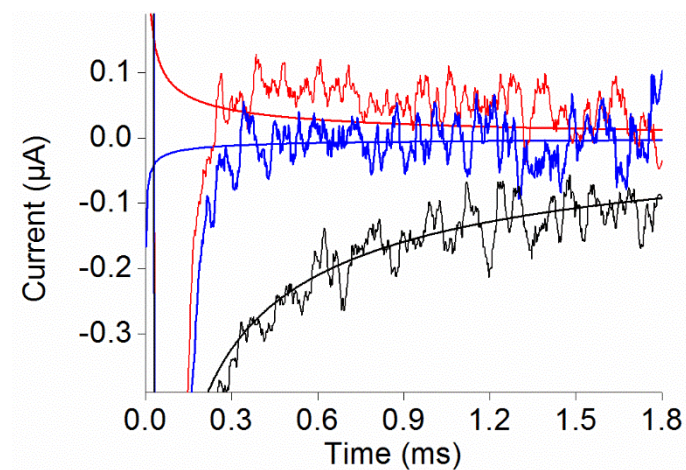


Figure S5. Oxidation of guanosine by $\text{Br}_2^{\bullet-}$. Transient electrochemical currents recorded at different potentials vs AgCl/Ag : 501 mV (black), 627 mV (blue), 641 mV (red). Solution composition: 1 mM guanosine, 0.1 M KBr, 0.1 M phosphate buffer under N_2O saturation. Dose: 10 Gy/pulse, corresponding to an initial concentration of 7.3 μM of **G(-H)•**.

1. M. S. Alam, E. Maisonhaute, D. Rose, A. Demarque, J. P. Larbre, J. L. Marignier and M. Mostafavi, *Electrochem. Commun.*, 2013, 35, 149-151.
2. J.-M. Saveant, *Elements of Molecular and Biomolecular Electrochemistry*, John Wiley and Son, Hoboken, New Jersey, first edn., 2006.
3. A. J. Bard and L. R. Faulkner, *Electrochemical Methods*, Wiley, New York, 2001.
4. Q. Li, C. Batchelor-McAuley and R. G. Compton, *J. Phys. Chem. B*, 2010, 114, 7423-7428.
5. Z. L. Wang, H. Kriegs and S. Wiegand, *J. Phys. Chem. B*, 2012, 116, 7463-7469.